Role of the Loop Containing Residue 115 in the Induced-Fit Mechanism of the Bacterial Cell Wall Biosynthetic Enzyme MurA‡

Ernst Schönbrunn,*,§,|| Susanne Eschenburg,⊥ Florian Krekel,§ Karolin Luger,|| and Nikolaus Amrhein§

Swiss Federal Institute of Technology, Institute of Plant Sciences, Universitätstrasse 2, CH-8092 Zürich, Switzerland, Colorado State University, Department of Biochemistry and Molecular Biology, Fort Collins, Colorado 80523, and Max-Planck Institute for Medical Research, Department of Biophysics, Jahnstrasse 29, D-69120 Heidelberg, Germany

Received May 13, 1999; Revised Manuscript Received December 6, 1999

ABSTRACT: The induced-fit mechanism in *Enterobacter cloacae* MurA has been investigated by kinetic studies and X-ray crystallography. The antibiotic fosfomycin, an irreversible inhibitor of MurA, induced a structural change in UDP-*N*-acetylglucosamine (UDPGlcNAc)-liganded enzyme with a time dependence similar to that observed for the inactivation progress. The mechanism of action of fosfomycin on MurA appeared to be of the bimolecular type, the overall rate constants of inactivation and structural change being $k^*_{inact} = 104\ M^{-1}\ s^{-1}$ and $k^*_{struc} = 85\ M^{-1}\ s^{-1}$, respectively. Fosfomycin as well as the second MurA substrate, phospho*enol*pyruvate (PEP), are known to interact with the side chain of Cys115. Like wild-type MurA, the catalytically inactive single-site mutant protein Cys115Ser structurally interacted with UDPGlcNAc in a rapidly reversible reaction. However, in contrast to wild-type enzyme, binding of PEP to mutant protein induced a rate-limited, biphasic structural change. Fosfomycin did not affect the structure of the mutant protein. The crystal structure of unliganded Cys115Ser MurA at 1.9 Å resolution revealed that the overall conformation of the loop comprising residues 112−121 is not influenced by the mutation. However, other than Cys115 in wild-type MurA, Ser115 exhibits two distinct side-chain conformations. A detailed view on the loop revealed the existence of an elaborate hydrogen-bonding network mainly supplied by water molecules, presumably stabilizing its conformation in the unliganded state. The comparison between the known crystal structures of MurA, together with the kinetic data obtained, suggest intermediate conformational states in the MurA reaction, in which the loop undergoes multiple structural changes upon ligand binding.

MurA (EC 2.5.1.7), the first enzyme of the bacterial cell wall biosynthetic pathway, catalyzes a mechanistically unusual reaction by transferring the intact *enol*pyruvyl moiety of phospho*enol*pyruvate (PEP)[1] to the 3-hydroxyl of UDP-*N*-acetylglucosamine (UDPGlcNAc) (ref *1*; Scheme 1). The enzyme is the target of the naturally occurring broad spectrum antibiotic fosfomycin [(1*R*,2*S*)-1,2-epoxypropyl phosphonic acid] (*2*). A similar reaction is catalyzed by EPSP synthase (EC 2.5.1.19), the sixth enzyme of the shikimate pathway, which is target of the broad-spectrum herbicide glyphosate (*3*).

In contrast to the reversible inhibition of EPSP synthase by glyphosate, fosfomycin inhibits MurA irreversibly by covalent attachment to the thiol group of a cysteine residue. This residue was identified as Cys115 in MurA from *Enterobacter cloacae* (*4*) and from *Escherichia coli* (*5*). The inactivation of *E. coli* MurA by fosfomycin was reported to be time dependent in a saturable manner, i.e., the formation of a rapidly reversible complex between MurA and fosfomycin is followed by covalent modification (*5*). Recently, it was demonstrated that the replacement of Cys115 with Asp115 in the *E. coli* enzyme results in catalytically competent enzyme. However, this mutant enzyme was no longer amenable to irreversible inhibition by fosfomycin (*6*). Since *Mycobacteria* naturally possesses Asp in position 115, this mutation is believed to be the major cause of fosfomycin resistance in *Mycobacteria* (*6*). Cys115 is the target of covalent modification not only by fosfomycin but also of the MurA substrate PEP, which reacts with this side chain to yield an O-phosphothioketal (*4*, *5*). However, the role of this covalent adduct in catalysis, if any, is not understood.

The crystal structures of MurA in the ligand-free (*7*) and UDPGLcNAc/fosfomycin-complexed forms (*8*) revealed that the reaction apparently follows an induced-fit mechanism in which the two-domain structure undergoes large conformational changes. The binding sites of UDPGlcNAc and fosfomycin are located in the cleft between the two globular domains, fosfomycin being covalently bound to the side chain of Cys115 (*8*). Cys115 is part of a loop which is solvent exposed in the open conformation, but forms a tight lid around the interdomain section in the closed conformation.

‡ The coordinates of unliganded Cys115Ser MurA have been deposited with the Brookhaven Protein Data Bank (accession code 1DLG).

* To whom correspondence should be addressed at Colorado State University. Phone: (970) 491-6571. Fax: (970) 491-0494. E-mail: eschoenb@lamar.colostate.edu.

§ Swiss Federal Institute of Technology.

|| Colorado State University.

⊥ Max-Planck Institute for Medical Research.

[1] Abbreviations: ANS, 8-anilino-1-naphthalene sulfonate; EPSP synthase, 5-*enol*pyruvyl-shikimate-3-phosphate synthase (EC 2.5.1.19); MurA, UDPGlcNAc *enol*pyruvyltransferase (EC 2.5.1.7); PEP, phospho*enol*pyruvate; UDPGlcNAc, uridine diphospho-*N*-acetyl-D-glucosamine.

10.1021/bi991091j CCC: $19.00
Published on Web 02/09/2000

Scheme 1

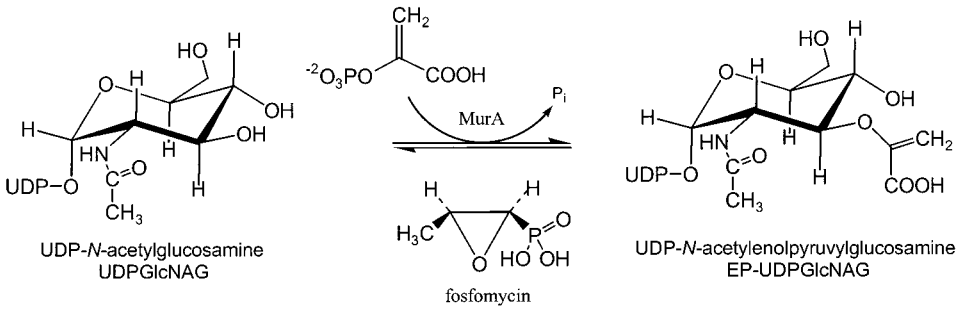

The closed MurA crystal structure is also known with a reaction intermediate analogue bound to the *E. coli* Cys115Ala mutant enzyme (*9*).

In contrast to the information available on its structure, little is known about the dynamics of this enzyme. Recently, solution studies on MurA revealed that the structural changes upon binding of ligands can be measured by the use of the extrinsic fluorophor ANS (*10*). The transition from the open to the closed form was shown to depend on the presence of UDPGlcNAc, consistent with the earlier interpretation of kinetic data that binding of substrates follows an ordered mechanism (*5*). PEP alone also induced structural changes in free enzyme, but these were different from the changes observed with the sugar nucleotide. Unlike the two substrates, fosfomycin did not affect the structure of free enzyme.

The applicability of ANS as a sensor to detect conformational changes in MurA prompted us to investigate ligand-induced changes of the MurA·UDPGLcNAc complex. Here, data obtained with *E. cloacae* MurA are presented from which we conclude that fosfomycin-induced inactivation and structural change are parallel processes. Both inactivation and structural change apparently follow a one-step mechanism, i.e., no rapidly reversible complex between enzyme and fosfomycin appears to be formed; the inhibitor rather appears to interact with the enzyme by way of a bimolecular reaction. Furthermore, we present evidence that the catalytically inactive Cys115Ser mutant protein is still capable of structural changes upon binding of UDPGlcNAc and PEP, but not of fosfomycin. However, the dynamic properties of the mutant protein upon PEP-binding are different from those of the wild-type enzyme. The role of the Cys115 containing loop in catalysis is discussed on the basis of the 1.9 Å resolution crystal structure of the open form of the Ser115-substituted MurA in comparison to the other known MurA structures.

MATERIALS AND METHODS

Cloning, overexpression, and purification of wild-type and C115S *E. cloacae* MurA have been described (*11*, *12*). Prior to the last purification step, i.e., chromatography on yellow agarose (Sigma), the enzyme was incubated with 1 mM UDPGlcNAc for 5 min at 37 °C to ensure complete loss of PEP attached covalently to Cys115. Purified protein was transferred to 50 mM sodium/potassium phosphate buffer (pH. 6.9) containing 1 mM DTT using a PD-10 column (Pharmacia), and concentrated to 20 mg/mL in Centricon-30 devices (Amicon). Aliquots were frozen in liquid nitrogen and stored at −80 °C.

Protein concentration was determined using the Coomassie Reagent from Pierce with bovine serum albumin as a standard. UDP-*N*-acetyl*enol*pyruvylglucosamine reductase (MurB) was prepared as described (*12*). Concentration of MurB was measured at 463 nm. UDPGlcNAc sodium salt, fosfomycin disodium salt, PEP tri(cyclohexylammonium) salt, and ANS ammonium salt were from Sigma. Glucose oxidase (*Aspergillus niger*, 138 U/mg) was from Fluka. Fitting of kinetic data was performed with SigmaPlot (Jandel). Basically, the strategy of Schloss (*13*) was used for evaluation and interpretation of the kinetic data obtained.

Inactivation Experiments. MurA activity was measured spectrophotometrically at 20 °C with a Uvikon 933 (Kontron Instruments) in a modified continuous assay using MurB as coupling enzyme (*14*). To reduce the diaphorase activity of MurB, a glucose oxidase/glucose system was exploited. This resulted in a stable baseline prior to initiation of the MurA reaction. The assay mixture (1 mL) contained 50 mM Tris/HCl, pH 7.4, 50 mM KCl, 20 mM glucose, 0.25 mM NADPH, 1 μM MurB, 20 units of glucose oxidase, 1 mM PEP and 1 mM UDPGLcNAc. The reaction was started by addition of MurA (final concentration 20 μg/mL = 0.44 μM) and the decrease in NADPH absorbance was recorded at a wavelength of 340 nm. The specific activity of MurA using this assay was 3.2 units/mg. The Cys115Ser mutant enzyme was inactive.

For inactivation studies, MurA (240 μg/mL = 5.3 μM) was incubated with UDPGlcNAc and fosfomycin in 500 μL of 50 mM sodium/potassium-phosphate buffer, pH 6.9, and 1 mM DTT, and at various time intervals, aliquots (90 μL) were assayed for residual activity. Control experiments were conducted in the same way, revealing that MurA activity remained constant for up to 60 min. Activity was measured by determining the initial velocities of assay progress curves. However, because of preincubating enzyme with inhibitor prior to assay, progress curves were straight lines under all conditions. Residual activity, in percent of the control, $f(t)$, was plotted as a function of incubation time (t) and data were fitted to

$$f(t) = 100 \times e^{-k_{obs}t} \quad (1)$$

where k_{obs} is the observed first-order rate constant of inactivation at one fosfomycin concentration. Data sets at different concentrations of UDPGLcNAc were evaluated by plotting k_{obs} values vs fosfomycin concentration (I), and fitting data to

$$f(I) = k_{inact}I \quad (2)$$

where k_{inact} equals the inactivation constant at one UDPGlcNAc concentration, $f(I)$ being k_{obs}. The overall inactivation constant k^*_{inact} was determined by fitting the individual

k_{inact} values to

$$f(S_1) = \frac{k^*_{inact} S_1}{K_{d(S_1)} + S_1} \quad (3)$$

where $K_{d(S_1)}$ is the dissociation constant of the MurA·UDPGlcNAc complex.

Fluorescence Measurements. Fluorescence was measured at 20 °C with a Kontron SFM-25 spectrofluorimeter controlled via the Wind25 software from Kontron Instruments. The buffer used for all measurements was 50 mM sodium/potassium phosphate (pH 6.9) with 1 mM DTT. Fluorescence of ANS was excited at 366 nm, and emission spectra were recorded between 600 and 400 nm. The ANS concentration was 100 μM, the MurA concentration 140 μg/mL (=3 μM), and those of UDPGlcNAc, PEP, or fosfomycin were varied between 10 μM and 2 mM, as indicated in the text/figures.

The reaction of wild-type MurA and mutant protein with ANS proceeds fast, i.e., equilibrium is established in less than 15 s. The same holds for the interaction of ANS-liganded wild-type enzyme and that of mutant protein with UDPGlcNAc. The $K_{d(UDPGlcNAc)}$ for the Cys115Ser mutant enzyme was derived from ANS emission spectra as previously described for wild-type enzyme (*10*).

Time-dependent ANS fluorescence quenching was recorded at the emission wavelength of 475 nm. For data evaluation, the percentage of fluorescence quenching after addition of fosfomycin or PEP to enzyme preincubated with UDPGlcNAc was plotted as a function of time. In the case of fosfomycin addition to wild-type enzyme, data were fitted to

$$f(t) = F + (100 - F)e^{-k_{obs}t} \quad (4)$$

where F is the residual fluorescence intensity at infinite time (t) and k_{obs} is the observed first-order rate constant of fluorescence quenching. $f(t)$ is the percentage of fluorescence quenching; 100% is the fluorescence intensity at 475 nm before addition of fosfomycin to UDPGlcNAc liganded enzyme.

The determination of the overall rate constant of fosfomycin-induced fluorescence change, which is assumed to reflect the structural change (k^*_{struc}), was performed as described for the inactivation experiment, i.e., k_{obs} values were fitted to eq 2 and the resulting k_{struc} values were fitted to eq 3.

The time-dependent fluorescence quenching of Cys115Ser mutant protein induced by PEP was analyzed by fitting data to

$$f(t) = F_2 + (F_1 - F_2)e^{-k_{obs}t} \quad (5)$$

where F_1 and F_2 are the relative fluorescence intensities at zero time and infinite time, respectively. k_{obs} values were plotted as a function of PEP concentration (S_2) and data were fitted to

$$f(S_2) = \frac{k_{struc\_on} S_2}{K_{d(S_1S_2)} + S_2} \quad (6)$$

where k_{struc_on} is the apparent first-order rate constant of PEP-induced structural change at one given UDPGlcNAc concentration (S_1), and $K_{d(S_1S_2)}$ is the apparent dissociation constant for PEP-interaction with UDPGlcNAc-liganded mutant protein (see Scheme 7). The overall rate constant of structural change ($k^*_{struc\_on}$), as well as the overall dissociation constant for PEP interaction with UDPGlcNAc-liganded mutant protein [$K^*_{d(S_1S_2)}$], were determined by fitting the individual k_{struc_on} values to

$$f(S_1) = \frac{k^*_{struc\_on} S_1}{K^*_{d(S_1S_2)} + S_1} \quad (7)$$

Crystallographic Analysis of the Cys115Ser Mutant Enzyme. Crystallization was performed essentially as described previously (*15*). Briefly, Cys115Ser mutant protein in 50 mM sodium/potassium-phosphate buffer, pH 6.9, containing 2 mM DTT was concentrated to 80 mg/mL. Equal volumes of the protein solution were mixed with 0.6 M sodium/potassium-phosphate buffer (pH 6.5)/40 mM cyclohexylammonium phosphate, and hanging droplets were equilibrated against a reservoir containing 1 M sodium/potassium-phosphate buffer (pH 6.5). Crystals typically appeared within 3 days and reached their final size of approximately 0.2 × 0.3 × 0.4 mm^3 after two more days. Diffraction data were recorded from one flash cooled crystal (T = 120 K, N_2 gas generated by an Oxford cryo-system) at the Swiss-Norwegian beam line BM1 (ESRF, Grenoble, France) equipped with a Mar Image Plate Scanner (X-ray Research, Norderstedt, Germany). The wavelength was 0.8729 Å. Data reduction was performed with the HKL suite (*16*, Table 1). The refinement was performed with the *CNS program package* (*17*) using four rounds of molecular dynamics/minimization/restrained individual *B*-factor refinement according to standard procedures (Table 1). Data were refined against the model of un-liganded MurA [PDB entry 1NAW to 1.55 Å resolution (Eschenburg, S., and Schönbrunn, E., unpublished material)]. The resulting electron density maps ($F_o - F_c$, $2F_o - F_c$) were evaluated with O (*18*). Model validation with PROCHECK (*19*) and WHAT_CHECK (*20*) revealed 94.2% of all 838 residues of both monomers having dihedral angles within the most favored regions of the Ramachandran plot, 5.1% within additionally allowed regions, 0.4% in generously allowed regions, and two residues (residue Asn67 of both monomers) in disallowed regions.

The current model of unliganded mutant MurA contains ca. 100 water molecules more per monomer than in unliganded wild-type MurA, due to better X-ray data and closer inspection of the electron density maps. The criterion for water molecule identification was as follows: clear signals in the $F_o - F_c$ synthesis above 3σ and in the $2F_o - F_c$ synthesis above 1σ, if at least one potential hydrogen-bonding partner was available (i.e., the distance between the water molecule and partner was in the range 2.3−3.2 Å). During the last two refinement rounds, water molecules having *B*-values greater than 40 Å^2 were again checked for consistency. In general, water molecules with *B*-values above 50 Å^2 were discarded.

RESULTS AND DISCUSSION

Inactivation of MurA by Fosfomycin. When MurA is preincubated with the sugar nucleotide and fosfomycin, the activity decreases single-exponentially as a function of time.

Table 1: Values for the Highest Resolution Shell Are Given in Parentheses

data collection statistics		refinement statistics	
space group	*C*2	resolution range (Å)	15−1.9
unit cell dimensions		no. of reflections used in refinement	86 055
a	86.7	no. of reflections used for R_{free}	2595
b	155.5	R_{cryst}[b] (%)	17.3
c	83.3	R_{free}[c] (%)	19.8
β	91.8	protein atoms (non-hydrogen)	6286
molecules/asym. unit	2	water molecules	1017
wavelength (Å)	0.8729	phosphate ions	9
temp (K)	120	cyclohexylammonium ions	3
resolution range (Å)	15.0−1.9	mean *B*-factor (protein) (Å^2)	21.6
no. of resolution shells	15	mean *B*-factor (water) (Å^2)	36.7
measured reflections	703 604	rmsd[d] bond lengths (Å)	0.013
unique reflections	86 085	rmsd[d] bond angles (deg)	1.8
completeness (%)	99.2 (91.9)		
$\langle I/\sigma(I)\rangle$	35.8 (5.9)		
R_{sym}[a] (%)	3.3 (11.9)		

[a] $R_{sym} = \Sigma_h\Sigma_i|I_{hi} - I_h|/\Sigma_h I_{hi}$ where *h* are unique reflection indices. [b] $R_{cryst} = \Sigma|F_{obs} - F_{model}|/\Sigma F_{obs}$ where F_{obs} and F_{model} are observed and calculated structure factor amplitudes, respectively. [c] *R*-factor calculated for 3% randomly chosen reflections which were excluded from the refinement. [d] rmsd = root-mean-square deviations from ideal values.

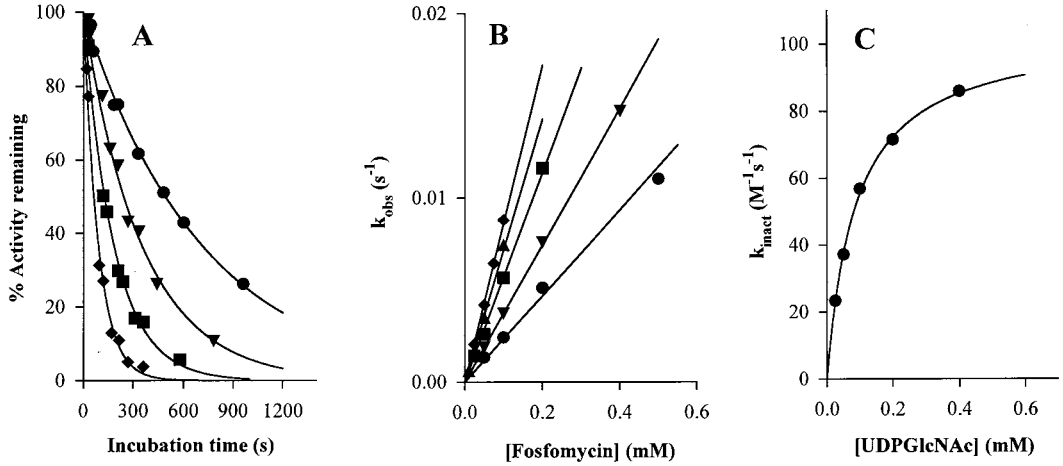

FIGURE 1: Inactivation of MurA by fosfomycin. (A) Time-dependent loss of MurA activity in the presence of 0.1 mM UDPGlcNAc. The fosfomycin concentration was 0.025 mM (●), 0.05 mM (▲), 0.1 mM (■) and 0.2 mM (◆). Data were fitted to eq 1 (solid lines). (B) Replot of the observed first-order rate constants of inactivation (k_{obs}) vs fosfomycin concentration for enzyme preincubated with various UDPGlcNAc concentrations [0.025 mM (●), 0.05 mM (▼), 0.1 mM (■), 0.2 mM (▲), and 0.4 mM (◆)]. Data were fitted to eq 2 (solid lines). (C) Replot of the second-order inactivation rate constants [k_{inact} (●)] vs UDPGlcNAc concentration. Data were fitted to eq 3 (solid lines) yielding k^*_{inact} = 104 ± 1.9 M^{-1} s^{-1} and $K_{d(UDPGlcNAc)}$ = 0.088 ± 0.004 mM.

Scheme 2

$$E + I \xrightarrow{k_{inact}} E\text{-}I$$

Figure 1A illustrates the inactivation of MurA in the presence of 0.2 mM UDPGlcNAc and increasing inhibitor concentrations. Data sets taken at five different UDPGlcNAc concentrations revealed a linear relationship between the observed first-order rate constants (k_{obs}) and fosfomycin concentration (Figure 1B). This is consistent with a mechanism lacking the formation of a rapidly reversible complex (EI). Thus, the inhibitor (I) covalently modifies its target (E) in a single step interaction (bimolecular type inhibition; Scheme 2).

The presence of UDPGlcNAc for inhibition is required (Figure 1C), i.e., fosfomycin binds to the rapidly reversible complex (ES_1) of free enzyme (E) and UDPGlcNAc (S_1). ES_1 then reacts with fosfomycin in a time-dependent manner, characterized by the overall rate constant k^*_{inact} to yield the dead-end complex, I-ES_1 (Scheme 3).

As evident from Figure 1C, the time-dependent process of inactivation is a function of UDPGlcNAc concentration

Scheme 3

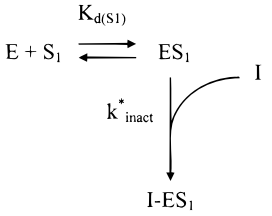

in a saturating manner. Fitting these data to eq 3 yields the second-order overall rate constant of inactivation, k^*_{inact} = 104 ± 1.9 M^{-1} s^{-1} . The dissociation constant of UDPGlcNAc [$K_{d(S_1)}$] is 0.088 ± 0.004 mM, which is similar to the dissociation constant derived from fluorescence measurements (0.059 mM, ref *10*), as well as to the K_m(UDPGlcNAc) of 0.053 mM (*12*).

Given the sluggish reactivity of epoxides, one would rather expect fosfomycin to initially bind in a reversible manner prior to the ring opening process. On the basis of preincubation studies on the inactivation of *E. coli* MurA by fosfomycin, an initially reversible inhibition at low fosfo-

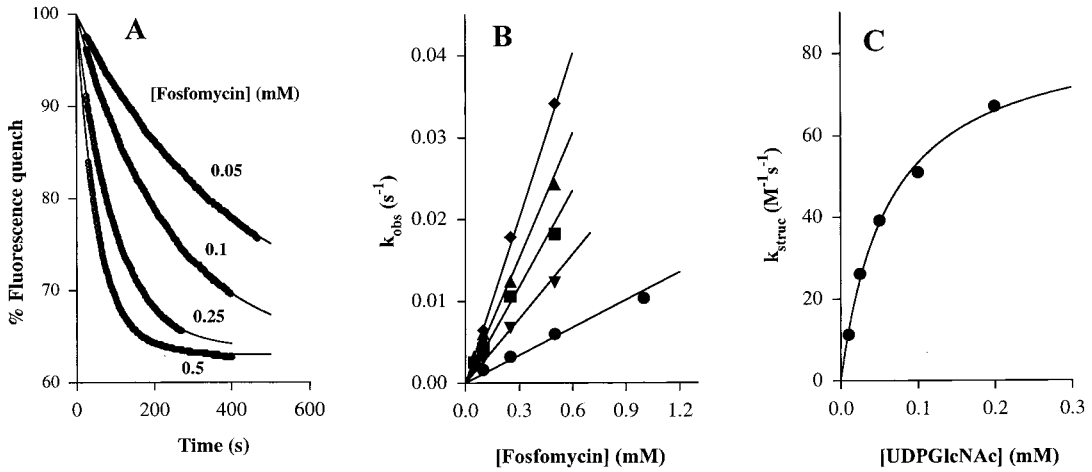

FIGURE 2: Fosfomycin-induced structural change in MurA. (A) Time-dependent fluorescence quenching of MurA/ANS emission spectra (●) in the presence of 0.05 mM UDPGlcNAc and increasing fosfomycin concentrations (0.05−0.5 mM). Excitation was at 366 nm; 100% is the emission maximum of UDPGlcNAc-liganded MurA at 475 nm prior to addition of fosfomycin. Data were fitted to eq 4 (solid lines). (B) Replot of the observed first-order rate constants of fluorescence change (k_{obs}) vs fosfomycin concentration for enzyme preincubated with various UDPGLcNAc concentrations [0.01 mM (●), 0.025 mM (▼), 0.05 mM (■), 0.1 mM (▲), and 0.2 mM (◆)]. Data were fitted to eq 2 (solid lines). (C) Replot of the second-order rate constants of structural change [k_{struc} (●)] vs UDPGlcNAc concentration. Data were fitted to eq 3 (solid line) yielding $k^*_{struc} = 86 \pm 4.4\ M^{-1}\ s^{-1}$ and $K_{d(UDPGlcNAc)} = 0.062 \pm 0.007$ mM.

Scheme 4

$$E + I \xrightarrow{k_{struc}} E\text{-}I$$

mycin concentrations was concluded ($K_i = 8.6\ \mu$M, ref *5*). In the present analysis of *E. cloacae* MurA, preincubation did not result in rate saturation for fosfomycin concentrations up to 0.5 mM. Because of the rapid inactivation process at fosfomycin concentrations above 0.5 mM, data cannot be measured accurately using the preincubation assay. However, an enzyme/inhibitor collision complex in *E. cloacae* MurA might occur at higher fosfomycin concentrations. A detailled kinetic analysis of the initial rate constants measured immediately upon inhibitor reaction is required to provide additional data on the mode of inactivation of MurA by fosfomycin.

Fosfomycin-Induced Fluorescence Changes. MurA is known to interact with the extrinsic fluorophor ANS in a manner allowing the characterization of structural changes upon ligand binding (*10*). While incubation of free enzyme with fosfomycin does not result in changes of the MurA/ANS emission spectra, the simultaneous presence of UDPGlcNAc induces a time-dependent fluorescence quench (Figure 2). Similar to the inactivation process, the k_{obs} values at each UDPGlcNAc concentration are directly proportional to the fosfomycin concentration (Figure 2B) consistent with a bimolecular type reaction. In this type of experiment, fosfomycin interaction with enzyme is characterized by a second-order rate constant of structural change, k_{struc} (Scheme 4).

Since only UDPGlcNAc-liganded enzyme is susceptible to fosfomycin binding and, furthermore, since k_{struc} as a function of UDPGlcNAc concentration varies in a saturating manner (Figure 2C), both the overall rate constant of structural change, k^*_{struc}, and the dissociation constant for UDPGlcNAc can be derived according to eq 3 and Scheme 5. The overall rate constant of the fosfomycin-induced structural change, k^*_{struc} is $85 \pm 4.4\ M^{-1}\ s^{-1}$, the derived K_d value for UDPGlcNAc binding is 0.062 ± 0.007 mM.

Scheme 5

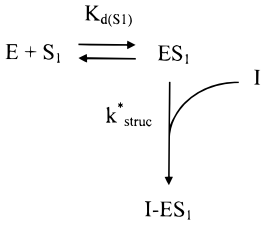

Scheme 6

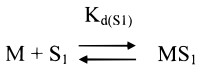

The conformity of the characteristic constants derived from the time-dependent inactivation assay and fluorescence measurements suggests a parallel event in inactivation and structural change. Moreover, as in the inactivation assay, rate saturation is not observed, underlying the one-step interaction mechanism of MurA and fosfomycin.

Dynamics of the Cys115Ser Mutant MurA. Fosfomycin covalently interacts with the side chain of Cys115 of *E. cloacae* MurA (*4*, *5*). Substituting Cys115 for serine results in catalytically inactive enzyme. However, this single-site mutant protein structurally interacts with UDPGlcNAc in a way similar to wild-type enzyme as determined by ANS-mediated fluorescence and small-angle X-ray scattering (data not shown). As for wild-type enzyme (*10*), the equilibrium between mutant protein (M) and UDPGlcNAc (S_1) is established rapidly, although the respective K_d value of 0.29 mM is four times higher than that of wild-type enzyme (Scheme 6).

The interaction of the mutant protein with either its second substrate PEP (S_2) or with fosfomycin (I) is fundamentally different from that observed with wild-type enzyme. PEP binds to free MurA in a rapidly reversible manner (*10*), whereas mutant protein reacts with PEP only in the presence of UDPGlcNAc (Figure 3). Unlike wild-type enzyme, which in complex with UDPGlcNAc reacts rapidly reversible with PEP (data not shown), the mutant protein undergoes time-

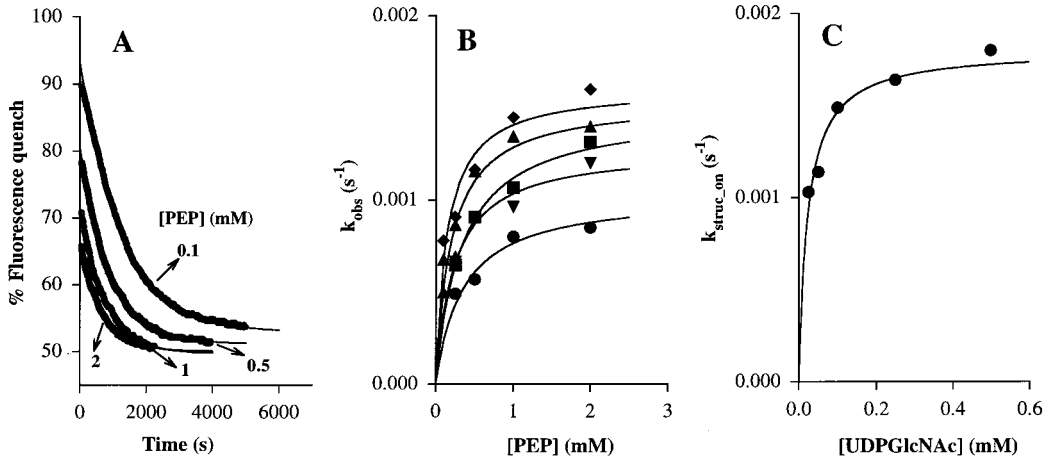

FIGURE 3: Rate-limited interaction between Cys115Ser MurA and PEP. (A) Time-dependent fluorescence quenching of Cys115Ser MurA/ANS emission spectra (●) in the presence of 0.25 mM UDPGLcNAc and increasing PEP concentrations (0.1−2 mM). Excitation was at 366 nm; 100% is the emission maximum of UDPGlcNAc-liganded mutant protein at 475 nm prior to addition of PEP. Data were fitted to eq 5 (solid lines). (B) Replot of the observed first-order rate constants of fluorescence change (k_{obs}) vs PEP concentration for enzyme preincubated with various UDPGlcNAc concentrations [0.025 mM (●), 0.05 mM (▼), 0.1 mM (■), 0.25 mM (▲), and 0.5 mM (◆)]. Data were fitted to eq 6 (solid lines). (C) Replot of the first-order rate constants of the onset of structural change [k_{struc_on} (●)] vs UDPGlcNAc concentration. Data were fitted to eq 7 (solid line) yielding $k^*_{struc\_on} = 1.82 \times 10^{-3} \pm 8.92 \times 10^{-5}$ s^{-1} and $K^*_{d(PEP/UDPGlcNAc)} = 0.023 \pm 0.0047$ mM.

dependent structural changes upon binding of PEP (Figure 3A). In contrast to fosfomycin-induced structural changes in wild-type enzyme (Figure 2), this interaction is of biphasic nature: a fast step (characterized by F_1 in eq 5) is followed by a time dependent step (k_{obs}) until a final level of fluorescence quench is established (F_2 in eq 5). This type of exponential decrease is consistent with a mechanism in which a rapidly reversible complex between UDPGlcNAc-liganded mutant protein (MS_1) and PEP (S_2) is formed (MS_1S_2) prior to the formation of a slowly reversible complex ($M^*S_1S_2$) (Scheme 7). The rate-determining step in PEP-induced

Scheme 7

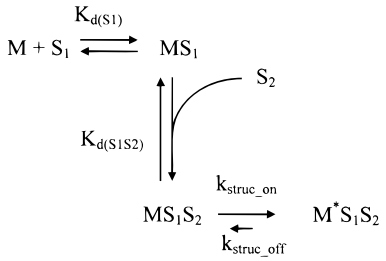

structural changes is characterized by k_{struc_on}. An equilibrium between the initial binary complex of enzyme−substrates interaction (MS_1S_2) and final conformation ($M^*S_1S_2$) is assumed, the ratio of k_{struc_off} and k_{struc_on} being much smaller than unity. The interaction of PEP with Cys115Ser mutant protein depends on the presence of UDPGlcNAc in a saturating manner (Figure 3c). Fitting these data to eq 7 gives an overall rate constant of PEP-induced structural changes ($k^*_{struc\_on}$) of $1.8 \times 10^{-3} \pm 9 \times 10^{-5}$ s^{-1}. The dissociation constant of PEP-binding to UDPGlcNAc-liganded mutant protein [$K_{d(S_1S_2)}$] is 0.02 ± 0.005 mM.

Fosfomycin-induced structural changes in free or UDPGlcNAc-liganded mutant protein are not observed, and the PEP-induced structural changes are not affected by fosfomycin (data not shown), corroborating the bimolecular type mechanism of inhibitor action. We therefore propose that fosfomycin should not be considered a ground-state analogue of PEP in the inactivation of wild-type *E. cloacae* MurA.

MurA is a two-domain protein known in two distinct forms: the unliganded, open state and the liganded, closed state (*7*−*9*; Figure 6). The kinetic data on wild-type enzyme and mutant protein provide evidence that the structural changes in MurA upon catalysis proceed by a mechanism involving at least two distinct conformational states of the enzyme: an intermediate structure with UDPGlcNAc bound to free enzyme followed by an end-state induced by fosfomycin or PEP. Cys115 appears to be activated upon binding of sugar nucleotide to free enzyme, possibly allowing fosfomycin to immediately interact with the thiol/thiolate group. The drastic effect of Cys115 mutation to Ser on ligand-induced structural changes prompted us to determine the crystal structure of unliganded mutant protein.

Investigation of the Loop Containing Ser115 by X-ray Crystallography. The crystal structure of Cys115Ser MurA is identical to that of wild-type enzyme. Superimposing the α-carbon chains of wild-type enzyme and mutant protein, the average deviation of all 838 structurally equivalent Cα atoms is 0.15 Å.

Residue 115 is part of a loop with the sequence Pro112-Gly-Gly-Cys-Ala-Ile-Gly-Ala-Arg-Pro121, which is solvent exposed in unliganded MurA (*7*). With the exception of the two alanine residues, and Cys115, which is replaced by Asp in *Mycobacteria*, this motif is highly conserved in all presently known MurA sequences (*12*). The loop is flanked by two strictly conserved hydrophobic residues, Leu111 and Val 122. Although the loop is, apart from the C-terminus, the most flexible part of the molecule with *B*-values of up to 40 Å^2 in Cα positions, its conformation is well-defined for the mutant protein by the electron density (Figure 4). Except for Gly113 and parts of the side chain of Pro121, clear density is visible at a contouring level of 1σ in the $2F_o - F_c$ map. The replacement of Cys115 by Ser does not alter the principle conformation of the loop. The rms deviation of the Cα-atoms of residues 111−123 of wild-type and

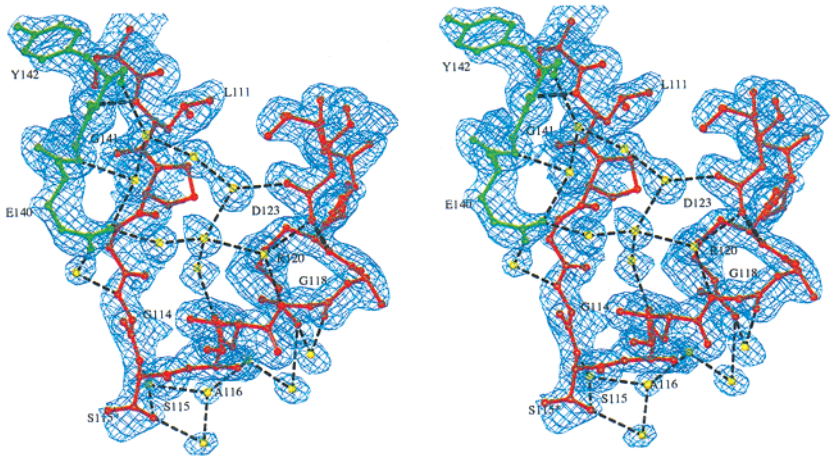

FIGURE 4: Hydrogen-bonding network stabilizing the loop around position 115 in unliganded Cys115Ser mutant MurA. Displayed is the final $2F_{obs} - F_{calc}$ stereo map contoured at 1σ around the loop containing Ser115 in momomer B. The view is from the top right of Figure 6 through the loop in the direction of the interdomain cleft. Presented are residues Leu111 to Asp123 (red), residues 140−142 (blue), and water molecules (yellow). Hydrogen bonds are indicated by dashed black lines. The two conformations of Ser115 are denoted Ser115* and Ser115. The figure was produced with O (*18*).

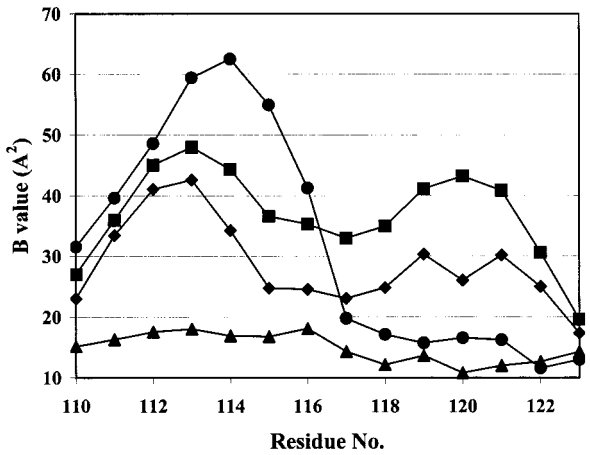

FIGURE 5: Conformational flexibility of the loop (I). *B*-value distribution of the Cα-atoms of residues 110−123 in unliganded Cys115Ser *E. cloacae* MurA (this work) (■), unliganded wild-type *E. cloacae* MurA [PDB entry 1NAW to 1.55 Å resolution (Eschenburg, S., and Schönbrunn, E., unpublished)] (◆), fosfomycin-liganded *E. coli* MurA [PDB entry 1UAE (*8*)] (▲), and intermediate state analog-liganded Cys115Ala *E. coli* MurA [PDB entry 1A2N, (*9*)] (●).

Ser115 mutant protein is only 0.3 Å. However, different from the side chain of Cys115 in wild-type enzyme, the side chain of Ser115 in mutant protein exhibits two distinct conformations. One of the Ser115 conformations follows the side-chain conformation of Cys115 in wild-type enzyme and protrudes into the solvent without hydrogen-bonding contacts. The side chain of the alternative serine conformation forms hydrogen bonds to two water molecules. One of these water molecules is part of a solvent chain bridging the hydroxyl group of Ser115 and the guanidinium group of Arg120. An elaborate solvent molecule network spans the loop and presumably stabilizes the solvent-exposed nature of the loop in the unliganded protein. The carboxyl group of the highly conserved side chain of Asp123 is involved in hydrogen-bonding contacts to the main-chain nitrogen of Arg120, as well as to two water molecules. Solvent chains of 11−14 Å in length connect Asp123 with main-chain atoms of Gly141 and Tyr142 and with a side-chain oxygen of Glu140. Thus, Asp123 appears to be the main anchor in the stabilization of the loop in unliganded MurA. In addition to the hydrogen-bonding network, the side chains of Leu111 and Val122 stay in hydrophobic interaction with each other, thereby acting as a spacer to separate the two sides of the loop.

The relative distribution of the *B*-values over the entire loop including the loop base is nearly the same for wild-type and Cys115Ser protein, i.e., an increase in value from the flanking residues Ser 110 to Gly114 and from Asp123 to Ala119 is followed by a decrease toward residue Ile117 (Figure 5) This relative minimum is presumably due to crystal contacts in form of a β-sheetlike interaction between residues 115 (C═O) to 118 (N) and symmetry-related residues 157 (N) to 159 (C═O). The crystal contacts of mutant protein and wild-type enzyme are identical and might influence the overall loop structure. In the absence of these crystal contacts, i.e., in solution, the loop is likely to adopt an even more flexible structure. Clearly, a second crystal form is needed to evaluate possible crystallization effects on the unliganded MurA structure. However, the base of the loop presumably reflects the true orientation in unliganded enzyme, given the above-described specific interactions of Asp123, and the Glu140−Tyr142 chain interaction with the loop, as well as the hydrophobic interaction of Leu111 and Val122.

Comparison of the Crystal Structures of Unliganded and Liganded MurA. Figure 6 displays the superposition of the crystal structure of Cys115Ser, representing MurA in its unliganded state ($MurA_{free}$), to the crystallographic models of UDPGlcNAc/fosfomycin-liganded MurA (PDB entry 1UAE; $MurA_{fosfomycin}$) and UDPGlcNAc/intermediate-state analogue liganded Cys115Ala (PDB entry 1A2N; $MurA_{intermediate}$). Apparently, the structural changes in MurA upon ligand binding involve both a movement of the upper N-terminal globular domain toward the interdomain section as well as additional conformational changes of the loop. While the loop of $MurA_{fosfomycin}$ fits tightly into the interdomain section, the loop of $MurA_{intermediate}$ is flexible in residues 113−115 (*9*), which is reflected in the *B*-value distribution (Figure 5). One side of the loop (residues 116−119) of both liganded forms is connected to the N-terminal

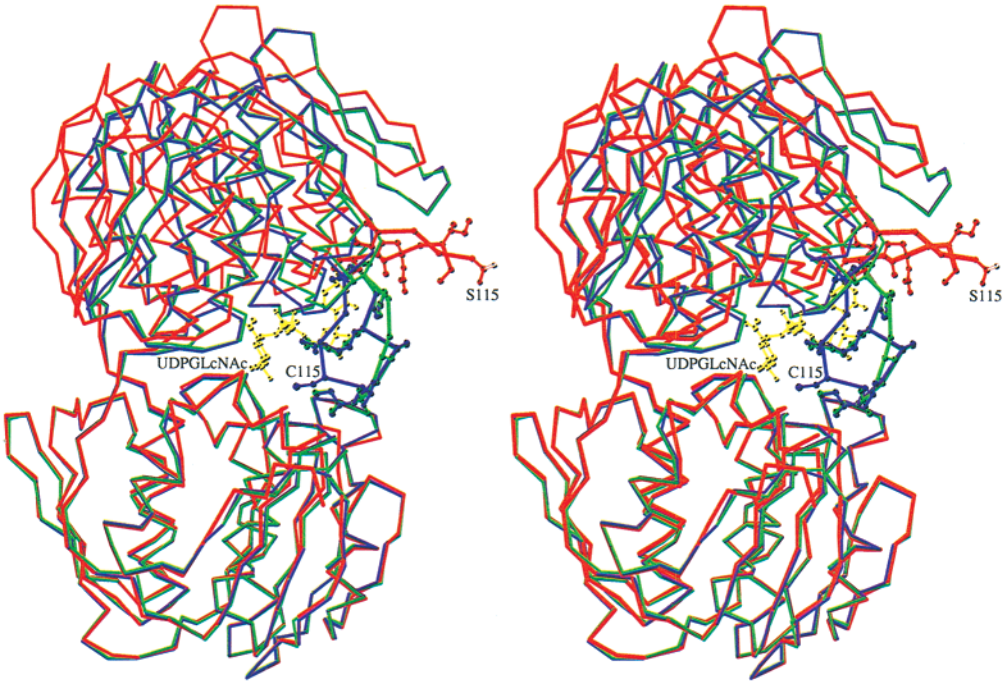

FIGURE 6: Comparison of the three known conformational states of MurA. Stereo plot of the Cα-chains of $MurA_{free}$ (red), $MurA_{fosfomycin}$ (blue), and $MurA_{intermediate}$ (green). The structures were aligned through the Cα-atoms of residues 300−400 belonging to the C-terminal (bottom) domain. The side chains of residues 112−121 are shown in ball-and-stick. High-lighted in yellow is UDPGlcNAc bound to $MurA_{fosfomycin}$ and $MurA_{intermediate}$.

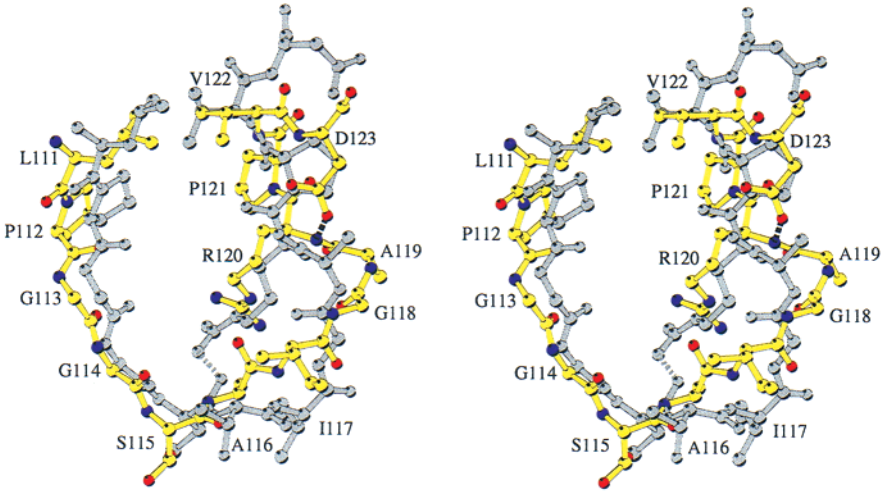

FIGURE 7: Conformational flexibility of the loop (II). Superposition of the loops of $MurA_{free}$ (yellow, atoms are shown in standard color) and $MurA_{fosfomycin}$ (grey). Hydrogen bonds are presented by black dashed lines. Alignment was performed through the Cα-atoms of residues 111−123. The view is approximately the same as in Figure 4.

globular domain through multiple hydrogen-bonding interactions to residues 329−330. Presumably, as a result of this loop attachment, main- and side-chain conformations of residues 329 and 330 differ considerably between unliganded and liganded MurA.

Superimposing the loops of $MurA_{free}$ and $MurA_{fosfomycin}$ reveals that the major differences in loop conformations reside in the C-terminal half of the loop (Figure 7). Upon ligand binding, Asp123 undergoes a large conformational change, and this event might initiate or trigger the loop inherent structural changes. Instead of anchoring the loop as described above, Asp123 interacts with UDPGlcNAc in both liganded structures. Moreover, in liganded MurA, the hydrophobic interaction between the flanking residues Leu111 and Val122 is disrupted, indicating that the arrangement of these two residues may be important for the structural changes in the loop. As a consequence of the side-chain rearrangements of Asp123 and Val122, the ring of Pro121 is free to rotate by nearly 180°, thereby altering the main-chain conformation of the successive loop residues.

Possible Role of Strictly Conserved Residues in the Establishment of the Catalytic Cavity. The structural events in the induced-fit mechanism of MurA involve a number of side-chain conformational rearrangements as a result of or as a prerequisite for creating the catalytic cavity. Figure 8 displays strictly conserved residues in a 5 Å radius around Cys115 in $MurA_{fosfomycin}$ with residues belonging to the C-terminal (bottom) domain of $MurA_{free}$ being superimposed. Arg91 is involved in interactions with loop inherent residues in $MurA_{fosfomycin}$, but not in $MurA_{intermediate}$ or ligand-free

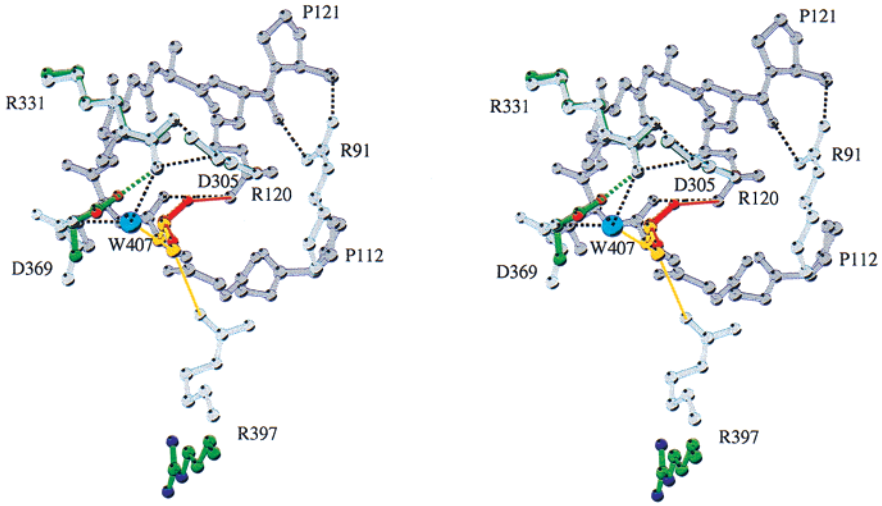

FIGURE 8: The probable function of strictly conserved residues in activating Cys115. Presented is a 5 Å radius around Cys115 including the entire loop of $MurA_{fosfomycin}$ (residues Pro112−Pro121); bound fosfomycin and UDPGlcNAc are omitted. The loop of $MurA_{fosfomycin}$ is shown in gray and its neighboring residues in light blue; the side chain of Cys115 is colored orange and the water molecule W407 in blue. Superimposed are residues Asp305, Arg331, Asp369, and Arg397 (green) of $MurA_{free}$. The alignment was performed as described in Figure 6. The introduced serine side chain in its two conformations is colored red. Hydrogen bonds in $MurA_{fosfomycin}$ are designated by black dotted lines, the salt bridge between Arg331 and Asp369 in $MurA_{free}$ is indicated by a green dashed line. Closest neighbors to the terminal group of Cys115 and to the introduced Ser115 are marked by yellow and red bold lines, respectively. Figures 6−8 were produced with Molscript (*22*).

protein. Since Arg91 binds to UDPGLcNAc only in the fosfomycin-liganded structure, this residue is possibly important for positioning the loop in the interdomain section upon the enzyme's reaction with either fosfomycin or PEP prior to the formation of the reaction intermediate.

The side chain of Asp305, involved in UDPGlcNAc-binding of both $MurA_{fosfomycin}$ and $MurA_{intermediate}$, and that of Arg331, which interacts with the intermediate state analogue in $MurA_{intermediate}$ only, do not change upon transition from the open to the closed state. Strictly conserved residues of the C-terminal globular domain in the vicinity of the catalytic site which undergo major conformational changes upon ligand binding are Arg397 and Asp369. Although Asp369 is not involved in binding of ligand(s), its conformational change might be important to the creation of an environment giving rise to the enhanced reactivity of Cys115. In unliganded wild-type and Cys115Ser mutant MurA, the carboxyl group of Asp369 establishes a salt-bridge with the guanidinium group of Arg331. In liganded MurA, this salt-bridge is broken and a water molecule (H_2O407 in 1UAE and 1A2N) is introduced, bridging the side chains of Asp369 and Arg331. Asp369 is highly conserved in MurA and in the structurally and mechanistically analogue EPSP synthase. Notably, substituting this residue for alanine in EPSP synthase, results in complete loss of catalytic activity (*21*).

The side chain of Arg397 is positioned parallel to the side chain of Lys48 in unliganded MurA. In the liganded structures, the side chain of Arg397 flips toward the interdomain section establishing a salt-bridge with Asp49 and at the same time forms hydrogen bonds to fosfomycin in 1UAE or to the fluoro-PEP moiety in $MurA_{intermediate}$. In $MurA_{fosfomycin}$, the thiol/thiolate group of Cys115 is only 3.4 Å distant from the guanidinum group of Arg397 and 3.2 Å from H_2O407. Since in $MurA_{fosfomycin}$ no other functional groups of protein or solvent are closer to the Cys115 side chain, Arg397 and this water molecule are the most likely candidates for the activation of Cys115. However, with 3.6 Å the distance between Cys115 of 1UAE and the carboxyl group of Asp369 in unliganded MurA is within a possible interaction between these two residues at some stage of the conformational changes associated with positioning Cys115 into the interdomain cleft.

Introducing the two serine rotamers of $MurA_{free}$ into position 115 of $MurA_{fosfomycin}$ reveals that one of the serine conformations resembles the side-chain conformation of Cys115 in $MurA_{fosfomycin}$. However, a comparable interaction as proposed above for the activation of Cys115 is not possible for Ser, since the resulting distances between the Ser115 hydroxyl group to H_2O407 and to the guanidinium group of Arg397 are too large to ensure a sufficient hydrogen bonding interaction**.** The second serine side-chain conformation would be sterically unfavorable because of a only 2.3 Å distance between its hydroxyl group and the guanidinium group of Arg120. Thus, the flexibility of the serine side chain as well as the smaller distance of the hydroxyl group to neighboring residues with respect to wild-type enzyme probably give rise to the slow structural changes upon PEP binding. Notably, an aspartate side chain introduced into position 115 of the fosfomycin-liganded MurA structure would fulfill the hydrogen-bonding contacts proposed to be important in the activation of Cys115 in wild-type enzyme. This might explain the catalytic efficiancy of the Cys115Asp *E. coli* mutant protein (*6*).

Concluding Remarks. Given the known crystal structures of MurA and the solution studies on the dynamics of this enzyme, a number of questions are still to be addressed to better understand the underlying induced-fit mechanism. For example, would the structure of MurA liganded with UDPGlcNAc alone resemble a state between the open and closed conformation, by which the enhanced reactivity of Cys115 could be explained? Is the structure of enzyme liganded with both substrates, prior to catalysis, similar to the fosfomycin inactivated or intermediate-state analogue

bound structure? In addition, does the enzyme perform opening and closing with each catalytic cycle or might it be that the open form is a resting state occurring only in the absence of UDPGlcNAc, whereas the enzyme remains in the closed form during catalysis until substrates have been depleted?

Its distinct structure and its essential role in bacteria makes MurA a valuable target for the development of novel antibiotics. In principle, any compound specifically inhibiting the conformational changes required to establish the catalytically active enzyme's form is a potentially useful antibacterial drug and, thus, may serve as a starting point for rational drug design.

ACKNOWLEDGMENT

We would like to thank the following collegues: Dr. K. Piontek (ETH Zürich, Switzerland) and his staff for making available their computer facilities, as well as Drs. T. Richmond and D. Sargent (ETH Hoenggerberg, Switzerland) for making available their X-ray facilities at the early stages of crystallographic measurements and refinement; Dr. K. Knudsen (SNBL/ESRF Grenoble, France) for support during the synchrotron experiment; Dr. J. V. Schloss (University of Kansas, USA) for discussions on the interpretation of the kinetic data.

REFERENCES

1. Walsh, C. T., Benson, T. E., Kim, D. H., and Lees, W. J. (1996) *Chem. Biol. 3*, 83−91.
2. Kahan, F. M., Kahan, J. S., Cassidy, P. J., and Kropp, H. (1974) *Ann. N. Y. Acad. Sci. 235*, 364−385.
3. Steinrücken, H. C., and Amrhein, N. (1980) *Biochem. Biophys. Res. Commun. 94*, 1207−1212.
4. Wanke, C., and Amrhein, N. (1993) *Eur. J. Biochem. 218*, 861−870.
5. Marquardt, J. L., Brown, D. E., Lane, W. S., Haley, T. M., Ichikawa, Y., Wong, C.-H., and Walsh, C. T. (1994) *Biochemistry 33*, 10646−10651.
6. Kim, D. H., Lees, W. J., Kempsell, K. E., Lane, W. S., Duncan, K., and Walsh, C. T. (1996) *Biochemistry 35*, 4923−4928.
7. Schönbrunn, E., Sack, S., Eschenburg, S., Perrakis, A., Krekel, F., Amrhein, N., and Mandelkow, E. (1996) *Structure (London) 4*, 1065−1075.
8. Skarzynski, T., Mistry, A., Wonacott, A., Hutchinson, S. E., Kelly, V. A., and Duncan, K. (1996) *Structure (London) 4*, 1465−1474.
9. Skarzynski, T., Kim, D. H., Lees, W. J., Walsh, C. T., and Duncan, K. (1998) *Biochemistry 37*, 2572−2577.
10. Schönbrunn, E., Svergun, D. I., Amrhein, N., and Koch, M. H. J. (1998) *Eur. J. Biochem. 253*, 406−412.
11. Wanke, C., Falchetto, R., and Amrhein, N. (1992) *FEBS Lett. 301*, 271−276.
12. Krekel, F. (1998) Dissertation ETH Zürich, Switzerland.
13. Schloss, J. V. (1989) in *Target sites of herbicide action* (Böger, P., and Sandmann, G., Eds.) pp 165−245, CRC Press, Boca Raton, FL.
14. Benson, T. E., Marquardt, J. L., Marquardt, A. C., Etzkorn, F. A., and Walsh, C. T. (1993) *Biochemistry 33*, 2024−2030.
15. Sack, S., Dauter, Z., Wanke, C., Amrhein, N., Mandelkow, E., and Schönbrunn, E. (1996) *J. Struct. Biol. 117*, 73−76.
16. Otwinowski, Z., and Minor, W. (1997) *Methods Enzymol. 276*, 307−326.
17. Brunger, A. T., Adams, P. D., Clore, G. M., DeLano, W. L., Gros, P., Grosse-Kunstleve, W., Jiang, J.-S., Kuszewski, J., Nilges, M., Pannu, N. S., Read, R. J., Rice, L. M., Simonson, T., and Warren, G. L. (1998) *Acta Crystallogr., Sect. D 54*, 905−921.
18. Jones, T. A., Zou, J.-Y., Cowan, S. W., and Kjeldgaard, M. (1991) *Acta Crystallogr., Sect. A 47*, 110−119.
19. Collaborative Computational Project, No. 4 (1994) *Acta Crystallogr., Sect. D 50*, 760−763.
20. Hooft, R. W. W., Vriend, G., Sander, C., and Abola, E. E. (1996) *Nature 381*, 272.
21. Shuttleworth, W. A., Pohl, M. E., Helms, G. L., Jakeman, D. L., and Evans, J. N. S. (1999). *Biochemistry 38*, 296−302.
22. Kraulis, P. J. (1991) *J. Appl. Crystallogr. 24*, 946−950.

BI991091J